



## Molecular fingerprints and health risks of smoke from home-use incense burning

Kai Song<sup>1,2,★</sup>, Rongzhi Tang<sup>3,4,★</sup>, Jingshun Zhang<sup>5</sup>, Zichao Wan<sup>1</sup>, Yuan Zhang<sup>6</sup>, Kun Hu<sup>1</sup>, Yuanzheng Gong<sup>1</sup>, Daqi Lv<sup>1</sup>, Sihua Lu<sup>1</sup>, Yu Tan<sup>7</sup>, Ruifeng Zhang<sup>3,4</sup>, Ang Li<sup>8</sup>, Shuyuan Yan<sup>8</sup>, Shichao Yan<sup>8</sup>, Baoming Fan<sup>9</sup>, Wenfei Zhu<sup>10</sup>, Chak K. Chan<sup>3,4</sup>, Maosheng Yao<sup>1</sup>, and Song Guo<sup>1,2</sup>

<sup>1</sup>State Key Joint Laboratory of Environmental Simulation and Pollution Control, International Joint Laboratory for Regional Pollution Control, Ministry of Education (IJRC), College of Environmental Sciences and Engineering, Peking University, Beijing 100871, China

<sup>2</sup>Collaborative Innovation Center of Atmospheric Environment and Equipment Technology, Nanjing University of Information Science & Technology, Nanjing 210044, China

<sup>3</sup>School of Energy and Environment, City University of Hong Kong, Kowloon 999077, Hong Kong SAR, China

<sup>4</sup>Shenzhen Research Institute, City University of Hong Kong, Shenzhen 518057, China

<sup>5</sup>Department of Investigation, Shanghai Police College, Shanghai 200137, China

<sup>6</sup>School of Earth Science and Engineering, Hebei University of Engineering, Handan 056038, China

<sup>7</sup>School of Chemical Engineering and Technology, Sun-Yat-Sen University, Zhuhai 519000, China

<sup>8</sup>China Automotive Technology and Research Center (CATARC), Beijing 100176, China

<sup>9</sup>TECHSHIP (Beijing) Technology Co., LTD, Beijing 100039, China

<sup>10</sup>School of Energy and Power Engineering, University of Shanghai for Science and Technology, Shanghai 200093, China

★These authors contributed equally to this work.

**Correspondence:** Rongzhi Tang (rongtang@cityu.edu.hk) and Song Guo (songguo@pku.edu.cn)

Received: 6 June 2023 – Discussion started: 13 June 2023

Revised: 29 July 2023 – Accepted: 21 August 2023 – Published: 1 November 2023

**Abstract.** The burning of incense for home use is a widespread practice that has been shown to have significant negative impacts on human health and air quality. However, there is a lack of understanding regarding its emission profiles and associated health risks. To address this knowledge gap, we utilized a state-of-the-art thermal-desorption comprehensive two-dimensional gas chromatography–mass spectrometer (TD-GC × GC-MS) to (semi-)quantify the emission factors (EFs) of 317 volatile compounds and thoroughly investigate the organic profiles of smoke from incense burning across a full-volatility range. Results showed that toluene ( $70.8 \pm 35.7 \mu\text{g g}^{-1}$ ) is the most abundant compound in smoke from incense burning, followed by benzene, furfural, and phenol. Phenol, toluene, furfural, 2-furanmethanol, benzene, and benzyl alcohol are the main contributors to ozone and secondary organic aerosol (SOA) estimation. Intermediate volatility organic compounds (IVOCs) accounted for 19.2 % of the total EFs but 40.0 % of the estimated SOA. Additionally, a novel pixel-based method, combined with aroma analysis, revealed that furfural can act as a key tracer of incense burning and is responsible for the distinctive aroma of incense smoke. High-bioaccumulation-potential (BAP) assessment using pixel-based partition coefficient estimation revealed that acenaphthylene, dibenzofuran, and phthalate esters (PAEs) are chemicals of high-risk concern and warrant further control. Our results highlight the critical importance of investigating home-use incense burning and provide new insights into the health impacts of smoke from incense burning using novel approaches.

## 1 Introduction

Incense burning is a prevalent custom in many cultures, especially in East and Southeast Asia (Chen et al., 2021). In modern times, incense burning for fragrance has become a frequent practice in households (Manoukian et al., 2013), while functional incense burning, such as mosquito coils, is used for specific purposes. Exposure to incense smoke is linked to adverse health effects like eye irritation, carcinogenicity, genotoxicity, and respiratory system damage (Wong et al., 2020; Yang et al., 2007, 2017). Incense is composed of fragrant materials, aromatic woods, herbs, and adhesive powders, usually available in the form of sticks and coils (Wong et al., 2020; Yadav et al., 2022). Incense burning releases multiple pollutants into the air, including particulate matter (PM), carbon monoxide (CO), volatile organic compounds (VOCs), and intermediate-volatility and semi-volatile organic compounds (I/SVOCs) (Wong et al., 2020; Yang et al., 2007; Jetter et al., 2002).

Current studies mainly focus on the hazardous VOC and SVOC homologues released from smoke from incense burning. For instance, Lee and Wang (2004) investigated 8 carbonyls and 11 VOCs emitted from incense burning and found that the emission factors (EFs) of traditional incense burning were higher than aromatic incense. Lu et al. (2020) detected 230 kinds of VOCs from mosquito-repellent incense burning, elucidating that alkanes, esters, aldehydes, ketones, and aromatics are predominant. Staub et al. (2011) measured 6 methoxy phenolics, 10 monoterpenoids, and 21 other kinds of SVOCs in the smoke from the burning of incense sticks and identified cedrol as an important odour source. However, most of the studies have focused on VOC compounds, with less attention given to gaseous organics in the full volatility range (VOCs–IVOCs–SVOCs). A full-volatility organic characterization may better evaluate the ozone formation potential (OFP) and SOA formation, as I/SVOCs are potentially important precursors of ozone and secondary organic aerosol (SOA) formation (Zhao et al., 2007; Tang et al., 2021; Guo et al., 2014, 2020). Meanwhile, mapping organics from incense smoke helps to evaluate the potential health risks of toxic compounds.

Comprehensive two-dimensional gas chromatography (GC × GC) is a powerful technique dealing with the coelution problem in conventional one-dimensional gas chromatography (1D GC). Pollutants from gasoline exhaust, diesel exhaust, and cooking emissions are separated and identified well (Drozd et al., 2019; Alam et al., 2018; Song et al., 2022a). As much as 50%–98% of the total response in GC × GC chromatograms could be explained (Huo et al., 2021; Song et al., 2022b). Previous work identified 324 compounds from incense smoke by coupling solid-phase microextraction (SPME) with GC × GC, yet chemicals are not quantified (Tran and Marriott, 2007). Thus, a non-targeted and quantitative assessment of incense-burning emissions is currently lacking.

In this work, two types of incense sticks and three kinds of incense coils were burned in a steel chamber. Gaseous pollutants were trapped by Tenax TA desorption tubes and then analysed by a thermal-desorption comprehensive two-dimensional gas chromatography–mass spectrometer (TD-GC × GC-MS). Pixel-based multiway principal component analysis (MPCA) was utilized to identify markers of incense burning. A risk assessment of pollutants from incense-burning emissions was then evaluated using pixel-based approaches, and high-risk compounds related to incense burning were assessed.

## 2 Methodology

### 2.1 Sampling and instrumentation

Incense was purchased from the market, including four common incense sticks, two Thai incense sticks, one mosquito coil, and two incense coils (Fig. S1 in the Supplement). Incense could also be classified by their material, containing two aromatic coils, four aromatic sticks, one mosquito coil, one sandalwood stick, and one smokeless sandalwood stick (Fig. S1). Incense was burned in a stainless combustion chamber (1 m<sup>3</sup>). After ignition, the burning incense changed from flaming to smoldering. Each kind of incense was burned at least twice. Incense was weighed before and after combustion. Preconditioned Tenax TA desorption tubes (Gerstel 6 mm 97 OD, 4.5 mm ID glass tube) were utilized to trap organics with a sampling flow of 0.2 L min<sup>-1</sup>.

A comprehensive two-dimensional gas chromatography–quadrupole mass spectrometer (GC × GC-qMS, GC-MS TQ8050, Shimadzu, Japan) coupled with a thermal-desorption system (TDS 3 C506, Gerstel, Germany) was used for sample analysis. The desorption temperature was 280 °C. The cooled injection system (CIS) with a Tenax TA liner was held at 20 °C and ramped up to 320 °C once the gaseous sample was injected into GC columns. The column combination was SH–Rxi–1ms (first, 30 m × 0.25 mm × 0.25 μm) and BPX50 (second, 2.5 m × 0.1 mm × 0.1 μm). The modulation period was 6 s. See Table S1 in the Supplement and elsewhere (Song et al., 2022a) for more information.

### 2.2 Chemical identification, quantification, and 2D binning

A series of standard mixtures (2, 5, 10, 20, and 40 μmL<sup>-1</sup> in CH<sub>2</sub>Cl<sub>2</sub>) was injected into Tenax TA tubes (2 μL). After purging the solvent with nitrogen gas, the standards were thermally desorbed. The standard mixture contains 26 *n*-alkanes (C7–C32, CNW Technologies, ANPEL Laboratory Technologies (Shanghai) Inc., China), 16 PAHs, 11 phenolic compounds, 9 alcohols, 4 aldehydes, 8 aromatics, 24 esters, 7 ketones, 5 siloxanes, and 39 other compounds. Gaseous organics are quantified by external calibration curves, with

most of the  $R$  squared ( $R^2$ ) values between 0.95 and 0.999 (Table S2). Chemicals with the same retention times and mass spectra were directly qualified and quantified. The unidentified chemicals were qualified by matching their mass spectrum with library spectra in the National Institute of Standard Technology library (NIST 17). Reverse factors of more than 700 were acceptable in this work. As homologues on the two-dimensional chromatogram (contour plot) were eluted with near-equal one-dimensional intervals, chemicals were then qualified by combining the location of the contour plot and the mass spectra (Song et al., 2023). Compounds without standards were semi-quantified by  $n$ -alkanes from the same volatility bin (uncertainty 69 %) and surrogates from the same chemical class (uncertainty 27 %). Instrument detection limits (IDLs) for organics semi-quantified were unknown; as a result, chemicals with negative values calculated by calibration curves were quantified by the volume-to-mass (ng) ratio of the lowest quantification point of standards (Table S2). A total of 317 chemicals were (semi)-quantified, including 10 acids, 34 alcohols, 19 aldehydes, 25 aromatics, 38 esters, 49 ketones, 18  $n$ -alkanes, 26 nitrogen-containing compounds, and 10 phenols (Table S3).

The compounds identified were sliced into two-dimensional bins (2D bins) (Song et al., 2022a). First retention times are linked to the volatility of species (B8 to B31 with decreasing volatility), while second retention times are associated with polarity (P1 to P8 with increasing polarity). Emission factors of compounds in the same 2D bin were aggregated (Table S3).

### 2.3 Emission factor (EF), ozone formation potential (OFP), and secondary organic aerosol (SOA) estimation

The emission factor (EF;  $\mu\text{g g}^{-1}$ ) was calculated by the following equation:

$$\text{EF} = \frac{m V}{f t M}, \quad (1)$$

where  $m$  is the absolute mass of pollutants ( $\mu\text{g}$ ) captured by Tenax TA tubes.  $V$  is the volume of the steel chamber ( $1 \text{ m}^3$ ). The sampling flow and duration of the Tenax TA tube are  $f$  ( $0.0002 \text{ m}^3 \text{ min}^{-1}$ ) and  $t$  (min), respectively.  $M$  is the combustion mass (g) of the incense. The sampling volume of Tenax TA tubes ( $0.003\text{--}0.01 \text{ m}^3$ ) was significantly smaller than the total volume of the steel chamber ( $1 \text{ m}^3$ ), and the volume change of the chamber could be neglected.

The ozone formation potential (OFP;  $\mu\text{g g}^{-1}$ ) was calculated using Eq. (2).  $\text{EF}_i$  is the emission factor of precursor  $i$  ( $\mu\text{g g}^{-1}$ ) with a maximum incremental reactivity (MIR) of  $\text{MIR}_i$ . The OFP was calculated inside the FOQAT packages developed by Tianshu Chen (<https://github.com/tianshu129/foqat>, last access: 10 August 2023). The MIR used in this work can be found in Table S3.

$$\text{OFP} = \sum [\text{EF}_i] \times \text{MIR}_i \quad (2)$$

Secondary organic aerosol (SOA) was estimated by Eq. (3).

$$\text{SOA} = \sum [\text{EF}_i] \times \left(1 - e^{-k_{\text{OH},i} \times [\text{OH}] \times \Delta t}\right) \times Y_i, \quad (3)$$

where  $k_{\text{OH},i}$  and  $Y_i$  represent the OH reaction rate and SOA yield of precursor  $i$ , respectively (Table S3). The SOA yields of precursors were from literature (Loza et al., 2014; Harvey and Petrucci, 2015; Tkacik et al., 2012; Shah et al., 2020; McDonald et al., 2018; Chan et al., 2010, 2009; Wu et al., 2017; Li et al., 2016; Matsunaga et al., 2009; Algrim and Ziemann, 2019, 2016; Liu et al., 2018; Charan et al., 2020) or surrogates from  $n$ -alkanes in the same volatility bins (Zhao et al., 2017).  $k_{\text{OH}}$  and  $Y$  can be found in Table S3.  $[\text{OH}] \times \Delta t$  is the OH exposure and was set to be  $13 \times 10^{10} \text{ molec. cm}^{-3} \text{ s}$  (24 h in OH concentration of  $1.5 \times 10^6 \text{ molec. cm}^{-3}$ ).

### 2.4 Pixel-based risk assessments of incense-burning pollutants

The octanol–air partition coefficient ( $K_{\text{o-a}}$ ), air–water partition coefficient ( $K_{\text{a-w}}$ ), and octanol–water partition coefficient ( $K_{\text{o-w}}$ ) were estimated using a linear free-energy relationship (LFER) model (Nabi et al., 2014; Zushi et al., 2019). Partition coefficients of chemicals are associated with their two-dimensional retention times (Song et al., 2022b). Chemicals with high bioaccumulation potential (BAP) are defined as contaminants with partition coefficients of ( $2 < \log K_{\text{o-w}} < 11$ ) and ( $6 < \log K_{\text{o-a}} < 12$ ). See Zushi et al. (2019) for more information. The R source code was obtained from GitHub (<https://github.com/Yasuyuki-Zushi>, last access: 10 August 2023).

## 3 Results and discussions

### 3.1 Emission profiles of different incense-burning organics

Figure S2 is a typical chromatogram of incense-burning emissions, which is also set as the reference chromatogram during the pixel-based analysis. As much as 90.2 % of the total response could be explained. The ratio is similar to a recent study resolving biomass-burning emissions (98 %) (Huo et al., 2021). The emission factor (EF) of total organics is  $791.8 \pm 300.6 \mu\text{g g}^{-1}$ , consistent with previous work ( $100\text{--}19100 \mu\text{g g}^{-1}$ ) (Lee and Wang, 2004) and comparable to rice ( $475.9 \pm 61.2 \mu\text{g g}^{-1}$ ), pine ( $558.6 \pm 103.6 \mu\text{g g}^{-1}$ ), and poplar ( $564.6 \pm 124.1 \mu\text{g g}^{-1}$ ) combustions (Zhu et al., 2022) but much lower than coal combustion ( $6.3 \text{ mg g}^{-1}$ ) (Huo et al., 2021). The contributions of different chemical categories are displayed in Fig. S3. Oxygenated compounds dominate the total EFs, accounting for 48.4 %, followed by aromatics (29.8 %),  $b$ -alkanes (5.3 %), nitrogen-containing compounds (4.0 %), alkenes (4.0 %), and  $n$ -alkanes (2.3 %). Unresolved complex mixtures (UCMs) are further separated into aliphatic, cyclic, and oxygenated UCM due to retention

times and mass spectra. The UCM ratio in this work (2.3 % in EFs) is comparable to biomass burning (Huo et al., 2021) and diesel exhaust (He et al., 2022) analysed by GC  $\times$  GC-MS and is much smaller than the UCM ratio ( $> 50\%$ ) in smoke from biomass burning analysed by 1D GC-MS (Zhu et al., 2022). Ketones are the most abundant oxygenated compounds, accounting for 13.6 % of the total EFs, followed by aldehydes (9.7 %), esters (8.1 %), alcohols (6.9 %), phenols (3.6 %), and acids (3.1 %). The emission profiles are comparable to corncob and wood combustion, which are also dominated by ketones and esters (Huo et al., 2021). However, the abundance of phenol is much lower than in smoke from biomass burning ( $> 15\%$ ) (Zhu et al., 2022; Huo et al., 2021), while it is comparable to coal combustion (5.4 %) (Huo et al., 2021).

EFs of selected compounds are listed in Table S4, and they are comparable with other incense-burning studies (Lee and Wang, 2004; Yang et al., 2007; Manoukian et al., 2016), while the EF of benzene ( $59.6 \pm 43.1 \mu\text{g g}^{-1}$ ) is slightly lower than other studies ( $188\text{--}1826 \mu\text{g g}^{-1}$ ) (Lee and Wang, 2004; Yang et al., 2007; Manoukian et al., 2016). The Tenax TA liner in the CIS system does not capture benzene at an initial temperature of  $20^\circ\text{C}$ , while it is efficient for the trapping of most I/SVOC compounds. A lower CIS temperature may trap benzene while causing water condensation. As a result, the tailing of benzene on the second column (Fig. S2) causes an underestimation of blob integration and results in an underestimation of EF.

The top-10 compounds are all VOC compounds (Fig. S4), accounting for 35.3 % of the total EFs. Toluene ( $70.8 \pm 35.7 \mu\text{g g}^{-1}$ ) is the most abundant compound in smoke from incense burning, followed by benzene, furfural, phenol, styrene, 2-oxo-propanoic acid methyl ester, 3-methyl-2-butanone, ethylbenzene, 1-hydroxy-2-propanone, and benzyl alcohol. Note that VOC compounds discussed here are part of volatile organics captured by Tenax-TA, not the common VOCs detected by SUMMA-GC-MS. The top-five IVOCs are B17 *b*-alkanes, B16 *b*-alkanes, B18 *b*-alkanes, diethyl phthalate, and 1,6-dioxacyclododecane-7,12-dione. The naphthalene (a typical PAH, two rings) EF is  $3.0 \pm 1.5 \mu\text{g g}^{-1}$ , comparable to rice straw combustion (Zhu et al., 2022). SVOCs are all *n*-alkane species and only account for less than 1 % of the total EFs.

The average volatility basis set (VBS) distribution of incense burning is displayed in Fig. 1, and the volatility–polarity distribution is exhibited in Fig. S5. In general, the EF decreases as the volatility decreases, following the trend of VOC EF (80.8 %)  $>$  IVOC EF (19.2 %)  $\gg$  SVOC EF ( $< 0.1\%$ ). The chemical compositions in the VOC–IVOC range are shown in Fig. S6. Oxygenated compounds (53.5 % of the total VOC EFs) and aromatics (37.6 %) are largely detected in the VOC range, while *b*-alkanes, *n*-alkanes, and oxygenated compounds are the main components of IVOC compounds. The average VBS distribution is similar to cooking emissions (Song et al., 2022a) and wood combustion

(Stewart et al., 2021) but less volatile than gasoline exhausts (Lu et al., 2018) and more volatile than diesel emissions (Lu et al., 2018). For example, the proportion of chemicals with saturated vapour concentration ( $C^*$ ) more than  $10^6 \mu\text{g m}^{-3}$  (Fig. 1a) is 80.8 % (incense burning), 80.7 % (cooking emissions) (Song et al., 2022a), 77.6 % (wood combustion) (Stewart et al., 2021), 94.2 % (gasoline exhaust) (Lu et al., 2018), and 41.0 % (diesel exhaust) (Lu et al., 2018). The polarity of incense burning is dominated by non-polar and intermediate-polarity organics (P1–P5, Fig. S5). The volatility–polarity distribution of incense burning is quite similar to cooking emissions (Song et al., 2022a), dominated by VOCs in the volatility range of before B13 and the polarity range of P1–P5.

A similar emission pattern but different EFs of different incense-burning emissions are observed. Similarities among incense burning are more dominant than diversities. First, pixel-based partial least squares–discriminant analysis (PLS-DA) elucidates that there is no systemic difference between different chromatograms of incense-burning emission, no matter different incense shapes (Fig. S7) or materials (Fig. S8). Second, the compositions of different types of incense emissions are indeed quite similar (Figs. S9 and S10). Third, the multiway principal component analysis (MPCA) positive loadings are much larger than negative loadings, indicating that the similarities between samples are much more important than the differences (Fig. 2).

However, the absolute EFs significantly diverge according to different incense forms ( $p = 0.03$ , Fig. S11) and different materials ( $p < 0.01$ , Fig. S12). Incense made in stick form (incense stick –  $893.2 \pm 335.6 \mu\text{g g}^{-1}$ ; Thailand incense stick –  $877.5 \pm 123.8 \mu\text{g g}^{-1}$ ) emits more organics than made in coil form (incense coil:  $835.5 \pm 306.0 \mu\text{g g}^{-1}$ ). The EF of mosquito coil is the smallest ( $382.5 \pm 175.0 \mu\text{g g}^{-1}$ ). A similar pattern was observed in previous work (Jetter et al., 2002). Concerning the incense materials, we spot that the so-called smokeless sandalwood stick emits more abundant organics ( $1195.8 \pm 83.3 \mu\text{g g}^{-1}$ ) than common sandalwood sticks ( $633.7 \pm 6.6 \mu\text{g g}^{-1}$ ). The emission of smokeless sandalwood sticks is even greater than aromatic sticks ( $893.2 \pm 335.6 \mu\text{g g}^{-1}$ ) and coils ( $824.8 \pm 228.5 \mu\text{g g}^{-1}$ ). Our results demonstrate that although smokeless sandalwood stick is preferred as fewer particulates are generated during the combustion process, the gaseous emissions are enhanced compared to other types of incense.

### 3.2 Contributions of home-use incense burning to ozone and secondary organic aerosols (SOAs)

The total OFP is  $1513.4 \pm 551.0 \mu\text{g g}^{-1}$ , which is  $1.91 \text{ g O}_3$  per g of VOCs–IVOCs. The OFP enhancement ratio (OFP per mass of precursor) is much smaller than gasoline exhaust ( $3.53 \text{ g O}_3$  per g of VOCs) (Wang et al., 2013) and evaporation ( $2.3\text{--}4.9 \text{ g O}_3$  per g of VOCs) (Yue et al., 2017), showing that incense burning is less efficient in ozone formation than

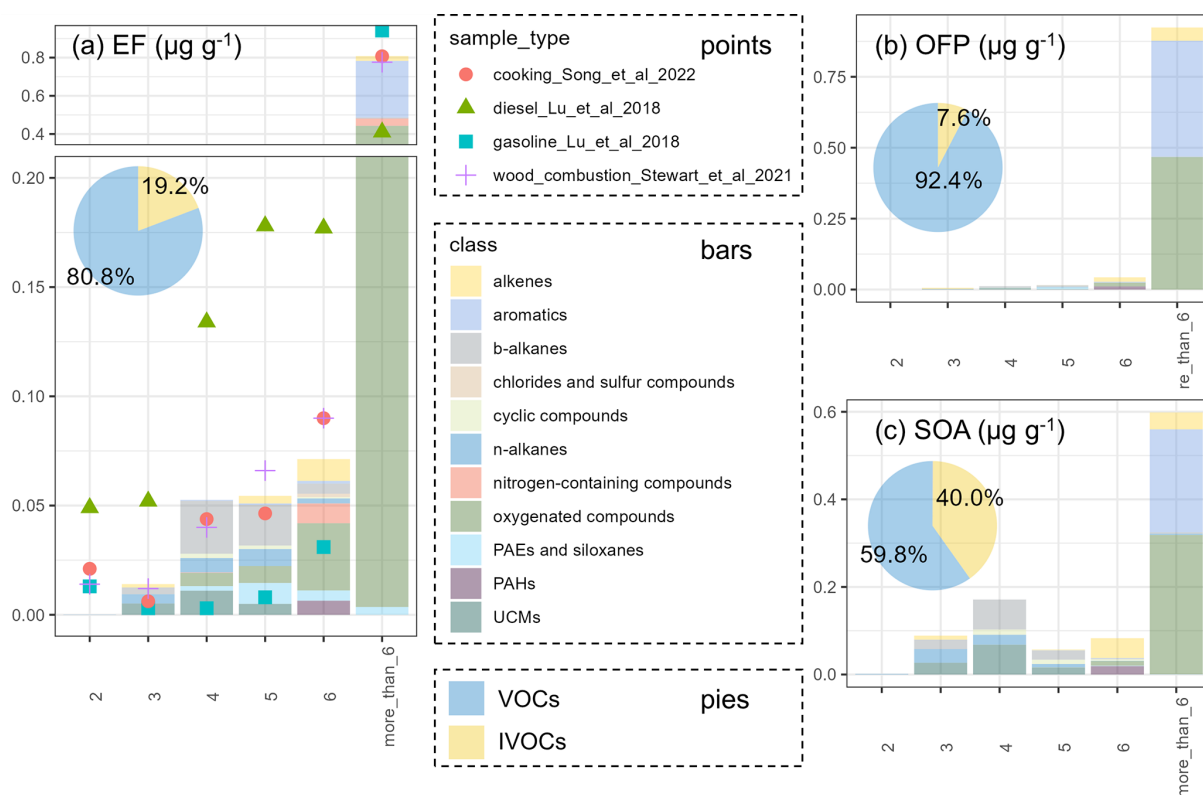


**Figure 1.** Volatility distributions of EF, OFP, and SOA with chemical class in each volatility bin. The  $x$  axis is the unsaturated vapour concentration in logarithmic form ( $\log C^*$ ,  $\mu\text{g m}^{-3}$ ). The  $y$  axis is the normalized mass emission factor (100 %).

gasoline-related sources. The lack of IVOC measurements in previous work could also cause an overestimation of the OFP enhancement ratio as IVOCs are less efficient in ozone formation. Toluene, furfural, *p*-xylene, benzyl alcohol, phenol, 2-furanmethanol, *o*-xylene, ethylbenzene, 1-hydroxy-2-propanone, and benzene are the top-10 species that contribute most to OFP (Fig. S4). Oxygenated compounds take up 48.2 % of the total OFP, followed by aromatics (41.0 %) and alkenes (6.7 %) (Fig. S3). VOCs dominate the total OFP, accounting for 92.4 %, while IVOCs take up 7.6 % (Fig. 1). Aromandendrene, naphthalene, and  $\alpha$ -cedrene are the top-three IVOC OFP contributors. The volatility distribution of OFP contribution is comparable to cooking emissions, as VOCs account for 88.8 %–99.9 % of the total cooking OFP estimation (Song et al., 2022a). Toluene contributes the most OFP in both cooking emissions and incense burning. Short-chain linear aldehydes (pentanal, hexanal, nonanal) originating from the degradation of oils play a more important role in OFP contribution in cooking emissions (Song et al., 2022a), while benzenes, furfural, alcohols, and phenols are non-negligible OFP contributors in incense burning.

Figure 1 shows the volatility distribution of estimated SOA estimation, with the top-10 contributors displayed in Fig. S4. IVOCs contribute 19.2 % of the EFs while accounting for 40.0 % of the total SOA estimation, highlighting the im-

portance of IVOCs in SOA formation. The contribution of IVOC species to SOA is higher than EFs due to the relatively higher yields and  $k_{\text{OH}}$ , which has already been reported in cooking emissions (Song et al., 2022a; Yu et al., 2022), gasoline exhaust (Zhao et al., 2014), diesel exhaust (Zhao et al., 2015), and biomass burning (Stewart et al., 2021). Oxygenated compounds account for 32.9 % of the SOA estimation, followed by aromatics (23.7 %), and *b*-alkanes (11.5 %) (Fig. S3). Phenol, benzyl alcohol, styrene, toluene, B18 cyclic UCM, aromandendrene, 2-furanmethanol, B17 *b*-alkanes, benzene, and phenylethyne are the top-10 SOA contributors. The incense-burning SOA formation profiles are distinct from cooking emissions (Song et al., 2022a) and biomass burning (Huo et al., 2021). Cooking SOA is largely derived from the oxidation of short-chain acids and aromatics (Song et al., 2022a), while phenols account for more than 65 % of the SOA estimation from biomass burning (Huo et al., 2021). Phenols only account for 11.0 % of SOA estimation in this work. Alcohols (7.3 %) and furans (7.6 %) are much more important SOA precursors in incense burning compared to biomass-burning and cooking emissions. Compared with other sources, we stress the importance of incense-burning benzenes, furfural, alcohols, and phenols in OFP formation and alcohols and furans in SOA formation. The secondary formation potential of mosquito coils is the

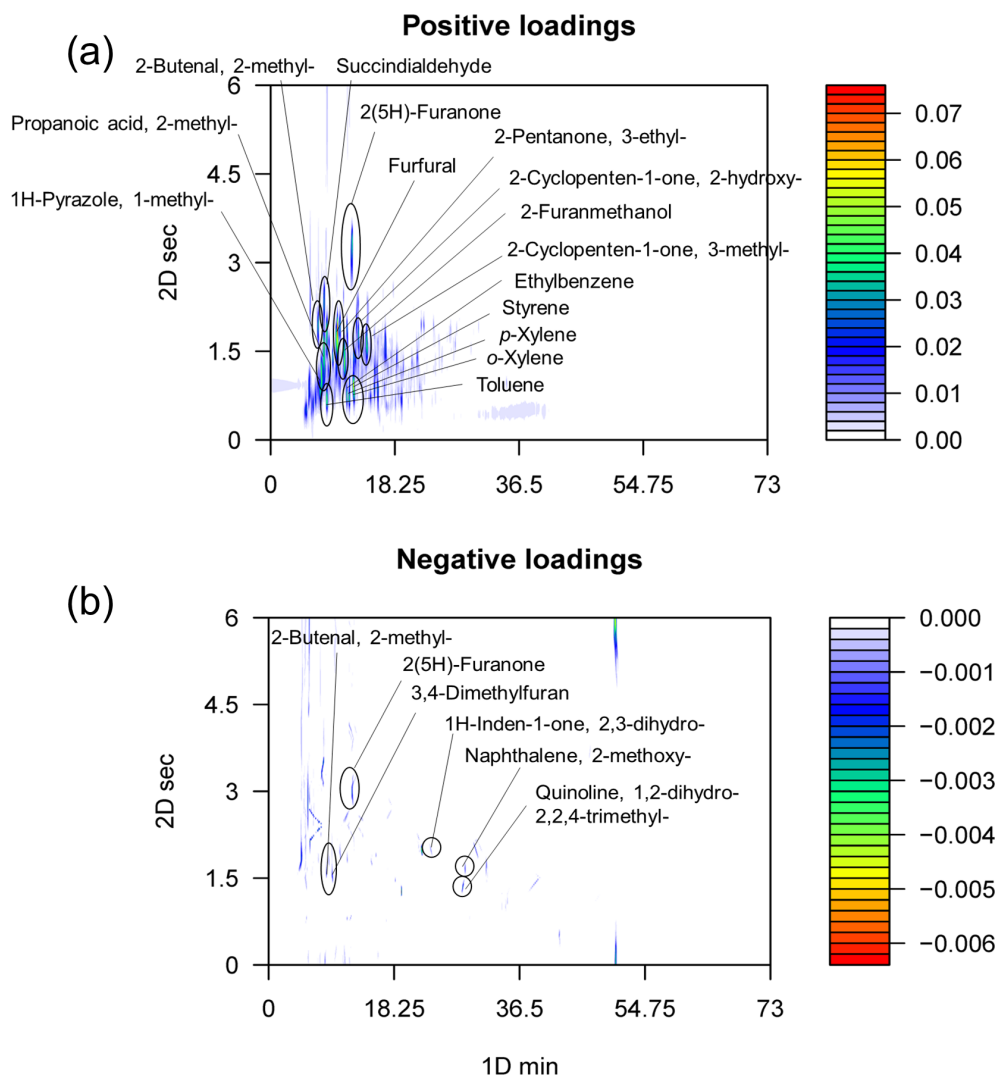


**Figure 2.** Positive (a) and negative (b) loadings of incense-burning samples, describing similarities and differences between chromatograms. The colour bar is the loading.

lowest, while the OFP and SOA of burning smokeless sandalwood sticks are the highest. Compared to other incense, the higher aromatic contents of smokeless sandalwood sticks burning fumes result in much more ozone and SOA formation.

### 3.3 Identification of molecular markers from incense burning

Pixel-based MPCA is utilized to identify tracers of incense-burning emissions. In brief, MPCA decomposes a matrix  $\mathbf{X}$  into a scoring matrix ( $\mathbf{S}$ ) and a loading matrix ( $\mathbf{L}$ ). Similarities and differences in chromatograms are revealed by positive and negative loadings, respectively (Fig. 2) (Song et al., 2022b). The similarities of chromatograms could be explained by benzenes (toluene, *p*-xylene, *o*-xylene, and ethylben-

zene), ketones (3-methyl-2-cyclopenten-1-one, 2-hydroxy-2-cyclopenten-1-one, 3-ethyl-2-pentanone), aldehydes (furfural, succinaldehyde, 2-methyl-2-butenal), 2-methylpropanoic acid, 1-methyl-1H-pyrazole, 2(5H)-furanone, and 2-furanmethanol. The differences between samples could be largely explained by 2-methyl-2-butenal, 2(5H)-furanone, 3,4-dimethylfuran, 2,3-dihydro-1H-inden-1-one, 2-methoxy-naphthalene, and 1,2-dihydro-2,2,4-trimethylquinoline. The negative loadings (0.006) are significantly smaller than the positive loadings (0.07), confirming the dominance of similarities among chromatograms. The relationship between the EFs of these compounds among different incense types is displayed in Fig. S13. Although the total EFs are significantly different ( $p = 0.03$ ), the EFs of selected compounds (2-hydroxy-2-cyclopenten-1-one, 2-furanmethanol, 3-ethyl-2-pentanone, and furfural) are significantly not different ( $p > 0.08$ ). As a result, we recom-

mend these compounds as incense-burning tracers. It is reported that furfural is formed during the thermal degradation of hemicelluloses (Uhde and Salthammer, 2007), while the oxidation of furfural under harsher conditions forms 2(5H)-furanone (Depoorter et al., 2021). The formation mechanism of furfural from xylose and *D*-xylopyranose is displayed in Fig. S14 (Ahmad et al., 1995; Bonner and Roth, 1959; Nimlos et al., 2006). The initiation of the degradation of five-carbon sugars is from the acyclic form of pentoses or directly via a 2,3-( $\alpha$ ,  $\beta$ )-unsaturated aldehyde. The dehydrating of the intermediate compounds finally forms furfural (Fig. S14). The addressed tracers, furfural, 2-furanmethanol, and 2(5H)-furanone, have already been identified in smoke from incense burning in previous work (Depoorter et al., 2021; Tran and Marriott, 2007).

Furthermore, we compare the chemical profiles with an odour database (Aroma Office 2D, Gerstel). Among the top-20 chemicals contributing to EFs, furfural (bread-like, alcoholic, incense-like), phenol (mushroom, acid, burnt plastics), 1-hydroxy-2-propanone (buttery, caramellic, fruity), benzyl alcohol (burning taste, flower, roasted), limonene (citrus-like, fruity, lemon-like), and 2-methyl-propanoic acid (apple-like, cheese-like, sweat) could be the aroma compounds. As for tracers identified above, 2-furanmethanol (burnt sugar, honey, sweet) could also be another aroma compound. Among them, furfural is widely and largely detected, which could be the most important molecular marker of incense burning (Silva et al., 2021; Ho and Yu, 2002). Note that aromandendrene, a cucumber-like, woody, and floral compound, is only detected in one incense coil sample (incense coil 2, Fig. S1). Aromandendrene is also detected in plants, such as in dry flowers of *Lonicera japonica* (Shang et al., 2011). The emission factor of aromandendrene is rather large ( $4.3 \mu\text{g g}^{-1}$ , 0.7 % of the total EFs) and is a significant SOA precursor ( $2.3 \mu\text{g g}^{-1}$ , 3.9 % of the total SOA estimation). The importance of aromandendrene in incense aroma and SOA formation could not be neglected. Aromandendrene could also be responsible for the distinct aroma of a certain incense coil. As mentioned above, we recommend furfural to be used as a molecular indicator of incense burning regardless of the incense type or additives, especially those responsible for the aroma of incense burning.

### 3.4 Risk assessment of incense-burning organics

The hazardous compounds from incense burning could cause adverse health effects on human health (Wong et al., 2020; Yang et al., 2007; Chen et al., 2021; Yang et al., 2017). To evaluate the potential risks of these compounds, we conducted a pixel-based risk assessment (bioaccumulation potential, BAP) for partition coefficient estimation. Chemicals with high-BAP concerns are listed in Fig. 3. 2-Methoxynaphthalene, acenaphthylene, dibenzofuran, diethyl phthalate, dibutyl phthalate, benzoic acid 2-ethylhexyl ester, C15–C19 *n*, and *b*-alkanes are regarded as high-BAP concerns

(Fig. 3). Among them, acenaphthylene is a toxic polycyclic aromatic hydrocarbon (PAH) that is widely detected in incense smoke (Yadav et al., 2022). Dibenzofuran, an oxygenated compound with detrimental effects on human health (Suzuki et al., 2021), is also detected in the smoke of incense burning (Tran and Marriott, 2007). Diethyl phthalate and dibutyl phthalate are phthalate esters (PAEs) widely used as plasticizers, which are endocrine disruptors (Wang and Qian, 2021). PAEs are abundant in incense smoke (Tran and Marriott, 2007). We propose that acenaphthylene, dibenzofuran, and PAEs could be chemicals of high-risk concern in incense smoke. We also assess the Arctic contamination potential (ACP) as shown in Sect. S1 in the Supplement. Further epidemiologic studies should be carried out to demonstrate the health effect of these hazardous compounds.

## 4 Implication

The non-target approach of GC  $\times$  GC-MS gives us a full glimpse of incense smoke, spotting a large pool of organics (317 compounds) covering the VOC–IVOC–SVOC range. We have provided a detailed description of both primary emission and secondary estimation of incense-burning organics which is ready to use in SOA simulation models. IVOCs (130 compounds) are crucial organics accounting for 19.2 % of the total EFs and 40.0 % of the SOA estimation, highlighting the importance of incorporating IVOCs into SOA models. Further investigation should be carried out to elucidate emission characteristics of short-chain compounds that are lacking in our research, such as alkanes (< C7), alkenes (< C7), and aldehydes (< C5). By combining data obtained from a gas chromatography–flame ionization detector (GC-FID) and a proton transfer mass spectrometer (PTR-MS), the emission pattern of incense burning could be demonstrated well. Comparisons of IVOC capture efficiency on different sampling materials should also be taken into account to obtain a reliable quantification result of IVOC species. High-time-resolution measurement should also be carried out to understand the time-resolved pattern of incense burning.

We also suggest furfural as the molecular marker of incense burning as the EFs of furfural among samples are relatively stable. Pixel-based MPCA also indicates that furfural is responsible for the similarities between chromatograms. Furfural may be the key aroma compound of incense smoke. This key component identified in this work could be implemented in source apportionment. Furfural is also a key component contributing to OFP (rank 2). Phenol, toluene, 2-furanmethanol, benzene, and benzyl alcohol are the main contributors to both OFP and SOA.

Surprisingly, we find that the EF of burning smokeless sandalwood sticks is the highest, with a remarkable contribution to OFP and SOA, due to the high aromatic contents. We recommend that both gaseous and particulate organics

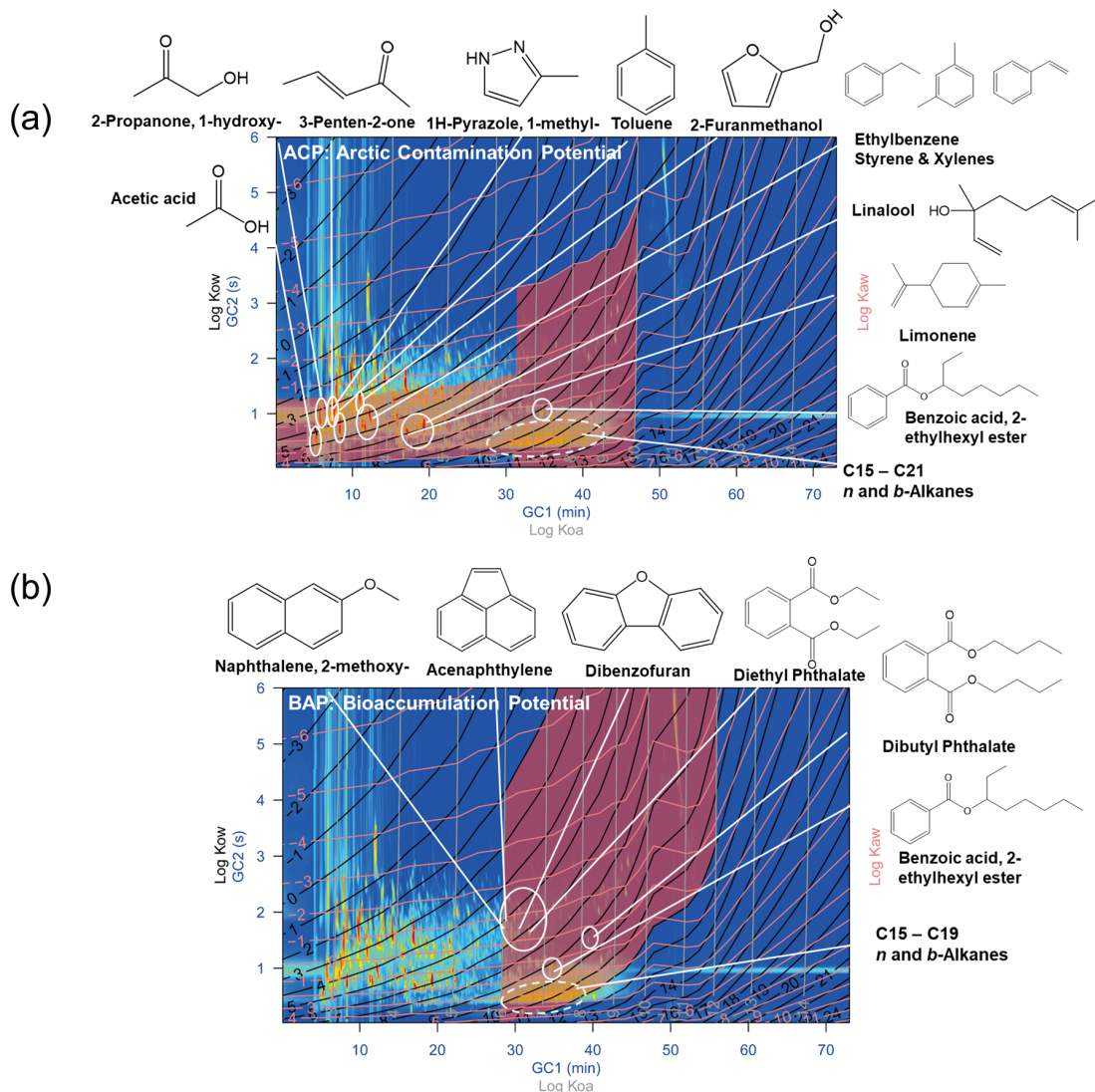


**Figure 3.** Chemicals with high bioaccumulation potential (BAP) assessed using pixel-based approaches.

should also be taken into consideration when burning incense. The single reduction of particles does not mean fewer emissions of gas-phase organics. A comprehensive assessment of incense-burning organics in both the gas and particle phase should be implemented.

Combining pixel-based property estimation and blob identification, the risk assessment analysis of compounds could benefit analysts with less experience with GC  $\times$  GC. The risk assessment in this work demonstrates that acenaphthylene, dibenzofuran, and PAEs are chemicals of high-risk concern and warrant further control. It was reported that more than half of Chinese residents have been burning incense every day at home for more than 20 years (Apte and Salvi, 2016). The toxic PAHs detected in indoor air could be 19 times higher than in outdoor air (Apte and Salvi, 2016). Exposure to these hazardous compounds could result in significant health threats. As a result, it is of vital importance to reveal

and assess the epidemiological influences of incense burning in future work.

**Code and data availability.** The code and data used in this publication can be accessed upon request to the corresponding authors (rongzhi.tang@cityu.edu.hk and songguo@pku.edu.cn).

**Supplement.** The supplement related to this article is available online at: <https://doi.org/10.5194/acp-23-13585-2023-supplement>.

**Author contributions.** KS and RT conducted the experiments. KS and RT analysed the data. All authors discussed the scientific results and reviewed the paper. KS, RT, and SG wrote the paper.

**Competing interests.** The contact author has declared that none of the authors has any competing interests.

**Disclaimer.** Publisher's note: Copernicus Publications remains neutral with regard to jurisdictional claims made in the text, published maps, institutional affiliations, or any other geographical representation in this paper. While Copernicus Publications makes every effort to include appropriate place names, the final responsibility lies with the authors.

**Acknowledgements.** The authors acknowledge the financial support of the National Natural Science Foundation of China, the National Key Research and Development Program of China, the National Science Foundation of Shandong Province of China, and the Hong Kong Research Grants Council.

**Financial support.** This research is supported by the National Natural Science Foundation of China (grant no. 22221004), the National Key Research and Development Program of China (grant no. 2022YFC3701000, Task 2), the National Natural Science Foundation of China (grant nos. 42107115, 41977179, 42275104), the National Science Foundation of Shandong Province, China (grant no. ZR2021QD111), and the Hong Kong Research Grants Council (grant no. 11304121).

**Review statement.** This paper was edited by Zhibin Wang and reviewed by two anonymous referees.

## References

- Ahmad, T., Kenne, L., Olsson, K., and Theander, O.: The formation of 2-furaldehyde and formic acid from pentoses in slightly acidic deuterium oxide studied by  $^1\text{H}$  NMR spectroscopy, *Carbohydr. Res.*, 276, 309–320, [https://doi.org/10.1016/0008-6215\(95\)00176-T](https://doi.org/10.1016/0008-6215(95)00176-T), 1995.
- Alam, M. S., Zeraati-Rezaei, S., Liang, Z., Stark, C., Xu, H., MacKenzie, A. R., and Harrison, R. M.: Mapping and quantifying isomer sets of hydrocarbons ( $\geq \text{C}_{12}$ ) in diesel exhaust, lubricating oil and diesel fuel samples using GC  $\times$  GC-ToF-MS, *Atmos. Meas. Tech.*, 11, 3047–3058, <https://doi.org/10.5194/amt-11-3047-2018>, 2018.
- Algrim, L. B. and Ziemann, P. J.: Effect of the Keto Group on Yields and Composition of Organic Aerosol Formed from OH Radical-Initiated Reactions of Ketones in the Presence of  $\text{NO}_x$ , *J. Phys. Chem. A*, 120, 6978–6989, <https://doi.org/10.1021/acs.jpca.6b05839>, 2016.
- Algrim, L. B. and Ziemann, P. J.: Effect of the Hydroxyl Group on Yields and Composition of Organic Aerosol Formed from OH Radical-Initiated Reactions of Alcohols in the Presence of  $\text{NO}_x$ , *ACS Earth Space Chem*, 3, 413–423, <https://doi.org/10.1021/acsearthspacechem.9b00015>, 2019.
- Apte, K. and Salvi, S.: Household air pollution and its effects on health, *F1000Research*, 5, 2593, <https://doi.org/10.12688/f1000research.7552.1>, 2016.
- Bonner, W. A. and Roth, M. R.: The Conversion of D-Xylose-1- $\text{C}^{14}$  into 2-Furaldehyde- $\alpha$ - $\text{C}^{14}$ , *J. Am. Chem. Soc.*, 81, 5454–5456, <https://doi.org/10.1021/ja01529a051>, 1959.
- Chan, A. W. H., Kautzman, K. E., Chhabra, P. S., Surratt, J. D., Chan, M. N., Crouse, J. D., Kürten, A., Wennberg, P. O., Flagan, R. C., and Seinfeld, J. H.: Secondary organic aerosol formation from photooxidation of naphthalene and alkylnaphthalenes: implications for oxidation of intermediate volatility organic compounds (IVOCs), *Atmos. Chem. Phys.*, 9, 3049–3060, <https://doi.org/10.5194/acp-9-3049-2009>, 2009.
- Chan, A. W. H., Chan, M. N., Surratt, J. D., Chhabra, P. S., Loza, C. L., Crouse, J. D., Yee, L. D., Flagan, R. C., Wennberg, P. O., and Seinfeld, J. H.: Role of aldehyde chemistry and  $\text{NO}_x$  concentrations in secondary organic aerosol formation, *Atmos. Chem. Phys.*, 10, 7169–7188, <https://doi.org/10.5194/acp-10-7169-2010>, 2010.
- Charan, S. M., Buenconsejo, R. S., and Seinfeld, J. H.: Secondary organic aerosol yields from the oxidation of benzyl alcohol, *Atmos. Chem. Phys.*, 20, 13167–13190, <https://doi.org/10.5194/acp-20-13167-2020>, 2020.
- Chen, K. S. F., Tsai, Y. P., Lai, C. H., Xiang, Y. K., Chuang, K. Y., and Zhu, Z. H.: Human health-risk assessment based on chronic exposure to the carbonyl compounds and metals emitted by burning incense at temples, *Environ. Sci. Pollut. R.*, 28, 40640–40652, <https://doi.org/10.1007/s11356-020-10313-1>, 2021.
- Depoorter, A., Kalalian, C., Emmelin, C., Lorentz, C., and George, C.: Indoor heterogeneous photochemistry of furfural drives emissions of nitrous acid, *Indoor Air*, 31, 682–692, <https://doi.org/10.1111/INA.12758>, 2021.
- Drozd, G. T., Zhao, Y., Saliba, G., Frodin, B., Maddox, C., Oliver Chang, M. C., Maldonado, H., Sardar, S., Weber, R. J., Robinson, A. L., Goldstein, A. H., Chang, M. C. O., Maldonado, H., Sardar, S., Weber, R. J., Robinson, A. L., Goldstein, A. H., Oliver Chang, M. C., Maldonado, H., Sardar, S., Weber, R. J., Robinson, A. L., and Goldstein, A. H.: Detailed Speciation of Intermediate Volatility and Semivolatile Organic Compound Emissions from Gasoline Vehicles: Effects of Cold-Starts and Implications for Secondary Organic Aerosol Formation, *Environ. Sci. Technol.*, 53, 1706–1714, <https://doi.org/10.1021/acs.est.8b05600>, 2019.
- Guo, S., Hu, M., Zamora, M. L., Peng, J., Shang, D., Zheng, J., Du, Z., Wu, Z., Shao, M., Zeng, L., Molina, M. J., and Zhang, R.: Elucidating severe urban haze formation in China, *P. Natl. Acad. Sci. USA*, 111, 17373–17378, <https://doi.org/10.1073/pnas.1419604111>, 2014.
- Guo, S., Hu, M., Peng, J., Wu, Z., Zamora, M. L., Shang, D., Du, Z., Zheng, J., Fang, X., Tang, R., Wu, Y., Zeng, L., Shuai, S., Zhang, W., Wang, Y., Ji, Y., Li, Y., Zhang, A. L., Wang, W., Zhang, F., Zhao, J., Gong, X., Wang, C., Molina, M. J., and Zhang, R.: Remarkable nucleation and growth of ultrafine particles from vehicular exhaust, *P. Natl. Acad. Sci. USA*, 117, 3427–3432, <https://doi.org/10.1073/pnas.1916366117>, 2020.
- Harvey, R. M. and Petrucci, G. A.: Control of ozonolysis kinetics and aerosol yield by nuances in the molecular structure of volatile organic compounds, *Atmos. Environ.*, 122, 188–195, <https://doi.org/10.1016/j.atmosenv.2015.09.038>, 2015.
- He, X., Zheng, X., You, Y., Zhang, S., Zhao, B., Wang, X., Huang, G., Chen, T., Cao, Y., He, L., Chang, X., Wang, S., and Wu, Y.: Comprehensive chemical characterization of gaseous I/SVOC emissions from heavy-duty diesel

- vehicles using two-dimensional gas chromatography time-of-flight mass spectrometry, *Environ. Pollut.*, 305, 119284, <https://doi.org/10.1016/j.envpol.2022.119284>, 2022.
- Ho, S. S. H. and Yu, J. Z.: Concentrations of formaldehyde and other carbonyls in environments affected by incense burning, *J. Environ. Monitor.*, 4, 728–733, <https://doi.org/10.1039/b200998f>, 2002.
- Huo, Y., Guo, Z., Liu, Y., Wu, D., Ding, X., Zhao, Z., Wu, M., Wang, L., Feng, Y., Chen, Y., Wang, S., Li, Q., and Chen, J.: Addressing Unresolved Complex Mixture of I/SVOCs Emitted From Incomplete Combustion of Solid Fuels by Nontarget Analysis, *J. Geophys. Res.-Atmos.*, 126, e2021JD035835, <https://doi.org/10.1029/2021JD035835>, 2021.
- Jetter, J. J., Guo, Z., McBrien, J. A., and Flynn, M. R.: Characterization of emissions from burning incense, *Sci. Total Environ.*, 295, 51–67, [https://doi.org/10.1016/S0048-9697\(02\)00043-8](https://doi.org/10.1016/S0048-9697(02)00043-8), 2002.
- Lee, S. C. and Wang, B.: Characteristics of emissions of air pollutants from burning of incense in a large environmental chamber, *Atmos. Environ.*, 38, 941–951, <https://doi.org/10.1016/j.atmosenv.2003.11.002>, 2004.
- Li, L., Tang, P., Nakao, S., and Cocker III, D. R.: Impact of molecular structure on secondary organic aerosol formation from aromatic hydrocarbon photooxidation under low-NO<sub>x</sub> conditions, *Atmos. Chem. Phys.*, 16, 10793–10808, <https://doi.org/10.5194/acp-16-10793-2016>, 2016.
- Liu, T., Wang, Z., Huang, D. D., Wang, X., and Chan, C. K.: Significant Production of Secondary Organic Aerosol from Emissions of Heated Cooking Oils, *Environ. Sci. Tech. Lett.*, 5, 32–37, <https://doi.org/10.1021/acs.estlett.7b00530>, 2018.
- Loza, C. L., Craven, J. S., Yee, L. D., Coggon, M. M., Schwantes, R. H., Shiraiwa, M., Zhang, X., Schilling, K. A., Ng, N. L., Canagaratna, M. R., Ziemann, P. J., Flagan, R. C., and Seinfeld, J. H.: Secondary organic aerosol yields of 12-carbon alkanes, *Atmos. Chem. Phys.*, 14, 1423–1439, <https://doi.org/10.5194/acp-14-1423-2014>, 2014.
- Lu, F., Li, S., Shen, B., Zhang, J., Liu, L., Shen, X., and Zhao, R.: The emission characteristic of VOCs and the toxicity of BTEX from different mosquito-repellent incenses, *J. Hazard. Mater.*, 384, 121428, <https://doi.org/10.1016/j.jhazmat.2019.121428>, 2020.
- Lu, Q., Zhao, Y., and Robinson, A. L.: Comprehensive organic emission profiles for gasoline, diesel, and gas-turbine engines including intermediate and semi-volatile organic compound emissions, *Atmos. Chem. Phys.*, 18, 17637–17654, <https://doi.org/10.5194/acp-18-17637-2018>, 2018.
- Manoukian, A., Quivet, E., Temime-Roussel, B., Nicolas, M., Maupetit, F., and Wortham, H.: Emission characteristics of air pollutants from incense and candle burning in indoor atmospheres, *Environ. Sci. Pollut. R.*, 20, 4659–4670, <https://doi.org/10.1007/s11356-012-1394-y>, 2013.
- Manoukian, A., Buiron, D., Temime-Roussel, B., Wortham, H., and Quivet, E.: Measurements of VOC/SVOC emission factors from burning incenses in an environmental test chamber: influence of temperature, relative humidity, and air exchange rate, *Environ. Sci. Pollut. R.*, 23, 6300–6311, <https://doi.org/10.1007/s11356-015-5819-2>, 2016.
- Matsunaga, A., Docherty, K. S., Lim, Y. B., and Ziemann, P. J.: Composition and yields of secondary organic aerosol formed from OH radical-initiated reactions of linear alkenes in the presence of NO<sub>x</sub>: Modeling and measurements, *Atmos. Environ.*, 43, 1349–1357, <https://doi.org/10.1016/j.atmosenv.2008.12.004>, 2009.
- McDonald, B. C., De Gouw, J. A., Gilman, J. B., Jathar, S. H., Akherati, A., Cappa, C. D., Jimenez, J. L., Lee-Taylor, J., Hayes, P. L., McKeen, S. A., Cui, Y. Y., Kim, S. W., Gentner, D. R., Isaacman-VanWertz, G., Goldstein, A. H., Harley, R. A., Frost, G. J., Roberts, J. M., Ryerson, T. B., and Trainer, M.: Volatile chemical products emerging as largest petrochemical source of urban organic emissions, *Science*, 359, 760–764, <https://doi.org/10.1126/science.aag0524>, 2018.
- Nabi, D., Gros, J., Dimitriou-Christidis, P., and Arey, J. S.: Mapping environmental partitioning properties of nonpolar complex mixtures by use of GC × GC, *Environ. Sci. Technol.*, 48, 6814–6826, <https://doi.org/10.1021/es501674p>, 2014.
- Nimlos, M. R., Qian, X., Davis, M., Himmel, M. E., and Johnson, D. K.: Energetics of xylose decomposition as determined using quantum mechanics modeling, *J. Phys. Chem. A*, 110, 11824–11838, <https://doi.org/10.1021/jp0626770>, 2006.
- Shah, R. U., Coggon, M. M., Gkatzelis, G. I., McDonald, B. C., Tasoglou, A., Huber, H., Gilman, J., Warneke, C., Robinson, A. L., and Presto, A. A.: Urban Oxidation Flow Reactor Measurements Reveal Significant Secondary Organic Aerosol Contributions from Volatile Emissions of Emerging Importance, *Environ. Sci. Technol.*, 54, 714–725, <https://doi.org/10.1021/acs.est.9b06531>, 2020.
- Shang, X., Pan, H., Li, M., Miao, X., and Ding, H.: *Lonicera japonica* Thunb.: Ethnopharmacology, phytochemistry and pharmacology of an important traditional Chinese medicine, *J. Ethnopharmacol.*, 138, 1–21, <https://doi.org/10.1016/j.jep.2011.08.016>, 2011.
- Silva, G. V., Martins, A. O., and Martins, S. D. S.: Indoor air quality: Assessment of dangerous substances in incense products, *Int. J. Env. Res. Pub. He.*, 18, 8086, <https://doi.org/10.3390/ijerph18158086>, 2021.
- Song, K., Guo, S., Gong, Y., Lv, D., Zhang, Y., Wan, Z., Li, T., Zhu, W., Wang, H., Yu, Y., Tan, R., Shen, R., Lu, S., Li, S., Chen, Y., and Hu, M.: Impact of cooking style and oil on semi-volatile and intermediate volatility organic compound emissions from Chinese domestic cooking, *Atmos. Chem. Phys.*, 22, 9827–9841, <https://doi.org/10.5194/acp-22-9827-2022>, 2022a.
- Song, K., Gong, Y., Guo, S., Lv, D., Wang, H., Wan, Z., Yu, Y., Tang, R., Li, T., Tan, R., Zhu, W., Shen, R., and Lu, S.: Investigation of partition coefficients and fingerprints of atmospheric gas- and particle-phase intermediate volatility and semi-volatile organic compounds using pixel-based approaches, *J. Chromatogr. A*, 1665, 462808, <https://doi.org/10.1016/j.chroma.2022.462808>, 2022b.
- Song, K., Guo, S., Gong, Y., Lv, D., Wan, Z., Zhang, Y., Fu, Z., Hu, K., and Lu, S.: Non-target scanning of organics from cooking emissions using comprehensive two-dimensional gas chromatography-mass spectrometer (GC × GC-MS), *Appl. Geochem.*, 151, 105601, <https://doi.org/10.1016/j.apgeochem.2023.105601>, 2023.
- Staub, P. O., Schiestl, F. P., Leonti, M., and Weckerle, C. S.: Chemical analysis of incense smokes used in Shaxi, Southwest China: A novel methodological approach in ethnobotany, *J. Ethnopharmacol.*, 138, 212–218, <https://doi.org/10.1016/j.jep.2011.08.078>, 2011.

- Stewart, G. J., Nelson, B. S., Acton, W. J. F., Vaughan, A. R., Hopkins, J. R., Yunus, S. S. M., Hewitt, C. N., Nemitz, E., Mandal, T. K., Gadi, R., Sahu, Lokesh. K., Rickard, A. R., Lee, J. D., and Hamilton, J. F.: Comprehensive organic emission profiles, secondary organic aerosol production potential, and OH reactivity of domestic fuel combustion in Delhi, India, *Environmental Science: Atmospheres*, 1, 104–117, <https://doi.org/10.1039/d0ea00009d>, 2021.
- Suzuki, S., Kiuchi, S., Kinoshita, K., Takeda, Y., Sakaida, S., Konno, M., Tanaka, K., and Oguma, M.: Formation of polycyclic aromatic hydrocarbons, benzofuran, and dibenzofuran in fuel-rich oxidation of toluene using a flow reactor, *Phys. Chem. Chem. Phys.*, 23, 6509–6525, <https://doi.org/10.1039/d0cp06615j>, 2021.
- Tang, R., Lu, Q., Guo, S., Wang, H., Song, K., Yu, Y., Tan, R., Liu, K., Shen, R., Chen, S., Zeng, L., Jorga, S. D., Zhang, Z., Zhang, W., Shuai, S., and Robinson, A. L.: Measurement report: Distinct emissions and volatility distribution of intermediate-volatility organic compounds from on-road Chinese gasoline vehicles: implication of high secondary organic aerosol formation potential, *Atmos. Chem. Phys.*, 21, 2569–2583, <https://doi.org/10.5194/acp-21-2569-2021>, 2021.
- Tkacik, D. S., Presto, A. A., Donahue, N. M., and Robinson, A. L.: Secondary organic aerosol formation from intermediate-volatility organic compounds: Cyclic, linear, and branched alkanes, *Environ. Sci. Technol.*, 46, 8773–8781, <https://doi.org/10.1021/es301112c>, 2012.
- Tran, T. C. and Marriott, P. J.: Characterization of incense smoke by solid phase microextraction-Comprehensive two-dimensional gas chromatography (GC × GC), *Atmos Environ*, 41, 5756–5768, <https://doi.org/10.1016/j.atmosenv.2007.02.030>, 2007.
- Uhde, E. and Salthammer, T.: Impact of reaction products from building materials and furnishings on indoor air quality-A review of recent advances in indoor chemistry, *Atmos. Environ.*, 41, 3111–3128, <https://doi.org/10.1016/j.atmosenv.2006.05.082>, 2007.
- Wang, J., Jin, L., Gao, J., Shi, J., Zhao, Y., Liu, S., Jin, T., Bai, Z., and Wu, C. Y.: Investigation of speciated VOC in gasoline vehicular exhaust under ECE and EUDC test cycles, *Sci. Total Environ.*, 445–446, 110–116, <https://doi.org/10.1016/j.scitotenv.2012.12.044>, 2013.
- Wang, Y. and Qian, H.: Phthalates and their impacts on human health, *Healthcare*, 9, 603, <https://doi.org/10.3390/healthcare9050603>, 2021.
- Wong, A., Lou, W., Ho, K.-f., Yiu, B. K.-f., Lin, S., Chu, W. C.-w., Abrigo, J., Lee, D., Lam, B. Y.-k., Au, L. W.-c., Soo, Y. O.-y., Lau, A. Y.-l., Kwok, T. C.-y., Leung, T. W.-h., Lam, L. C.-w., Ho, K., and Mok, V. C.-t.: Indoor incense burning impacts cognitive functions and brain functional connectivity in community older adults, *Scientific Reports*, 10, 7090, <https://doi.org/10.1038/s41598-020-63568-6>, 2020.
- Wu, W., Zhao, B., Wang, S., and Hao, J.: Ozone and secondary organic aerosol formation potential from anthropogenic volatile organic compounds emissions in China, *J. Environ. Sci.*, 53, 224–237, <https://doi.org/10.1016/j.jes.2016.03.025>, 2017.
- Yadav, V. K., Malik, P., Tirth, V., Khan, S. H., Yadav, K. K., Islam, S., Choudhary, N., Inwati, G. K., Arabi, A., Kim, D. H., and Jeon, B. H.: Health and Environmental Risks of Incense Smoke: Mechanistic Insights and Cumulative Evidence, *J. Inflamm. Res.*, 15, 2665–2693, <https://doi.org/10.2147/JIR.S347489>, 2022.
- Yang, T. T., Lin, T. S., and Chang, M.: Characteristics of emissions of volatile organic compounds from smoldering incense, *B. Environ. Contam. Tox.*, 78, 308–313, <https://doi.org/10.1007/s00128-007-9184-9>, 2007.
- Yang, T. T., Ho, S. C., Chuang, L. te, Chuang, H. C., Li, Y. T., and Wu, J. J.: Characterization of particulate-phase polycyclic aromatic hydrocarbons emitted from incense burning and their bioreactivity in RAW264.7 macrophage, *Environ. Pollut.*, 220, 1190–1198, <https://doi.org/10.1016/j.envpol.2016.11.016>, 2017.
- Yu, Y., Guo, S., Wang, H., Shen, R., Zhu, W., Tan, R., Song, K., Zhang, Z., Li, S., Chen, Y., and Hu, M.: Importance of Semivolatile/Intermediate-Volatility Organic Compounds to Secondary Organic Aerosol Formation from Chinese Domestic Cooking Emissions, *Environ. Sci. Tech. Lett.*, 9, 507–512, <https://doi.org/10.1021/acs.estlett.2c00207>, 2022.
- Yue, T., Yue, X., Chai, F., Hu, J., Lai, Y., He, L., and Zhu, R.: Characteristics of volatile organic compounds (VOCs) from the evaporative emissions of modern passenger cars, *Atmos. Environ.*, 151, 62–69, <https://doi.org/10.1016/j.atmosenv.2016.12.008>, 2017.
- Zhao, Y., Hu, M., Slanina, S., and Zhang, Y.: Chemical compositions of fine particulate organic matter emitted from Chinese cooking, *Environ. Sci. Technol.*, 41, 99–105, <https://doi.org/10.1021/es0614518>, 2007.
- Zhao, Y., Hennigan, C. J., May, A. A., Tkacik, D. S., de Gouw, J. A., Gilman, J. B., Kuster, W. C., Borbon, A., and Robinson, A. L.: Intermediate-volatility organic compounds: A large source of secondary organic aerosol, *Environ. Sci. Technol.*, 48, 13743–13750, <https://doi.org/10.1021/es5035188>, 2014.
- Zhao, Y., Nguyen, N. T., Presto, A. A., Hennigan, C. J., May, A. A., and Robinson, A. L.: Intermediate Volatility Organic Compound Emissions from On-Road Diesel Vehicles: Chemical Composition, Emission Factors, and Estimated Secondary Organic Aerosol Production, *Environ. Sci. Technol.*, 49, 11516–11526, <https://doi.org/10.1021/acs.est.5b02841>, 2015.
- Zhao, Y., Saleh, R., Saliba, G., Presto, A. A., Gordon, T. D., Drozd, G. T., Goldstein, A. H., Donahue, N. M., and Robinson, A. L.: Reducing secondary organic aerosol formation from gasoline vehicle exhaust, *P. Natl. Acad. Sci. USA*, 114, 6984–6989, <https://doi.org/10.1073/pnas.1620911114>, 2017.
- Zhu, X., Han, Y., Feng, Y., Cheng, P., Peng, Y., Wang, J., Cai, J., and Chen, Y.: Formation and emission characteristics of intermediate volatile organic compounds (IVOCs) from the combustion of biomass and their cellulose, hemicellulose, and lignin, *Atmos. Environ.*, 286, 119217, <https://doi.org/10.1016/j.atmosenv.2022.119217>, 2022.
- Zushi, Y., Yamatori, Y., Nagata, J., and Nabi, D.: Comprehensive two-dimensional gas-chromatography-based property estimation to assess the fate and behavior of complex mixtures: A case study of vehicle engine oil, *Sci. Total Environ.*, 669, 739–745, <https://doi.org/10.1016/j.scitotenv.2019.03.157>, 2019.